SPOP promotes cervical cancer progress by inducing PD-1 move away from PD-L1 in spatial localization

Jiangchun Wu
Shanghai Cancer Hospital: Fudan University Shanghai Cancer Center
Yong Wu
Shanghai Cancer Hospital: Fudan University Shanghai Cancer Center
Qinhao Guo
Shanghai Cancer Hospital: Fudan University Shanghai Cancer Center
Siyu Chen
Shanghai Cancer Hospital: Fudan University Shanghai Cancer Center
Simin Wang
Shanghai Cancer Hospital: Fudan University Shanghai Cancer Center
Jun Zhu
Shanghai Cancer Hospital: Fudan University Shanghai Cancer Center
Xiaohua Wu (wu.xh@fudan.edu.cn)
Fudan University Shanghai Cancer Center
Xingzhu Ju
Shanghai Cancer Hospital: Fudan University Shanghai Cancer Center

Research Article

Keywords: cervical cancer, SPOP, multiplex immunofluorescence

Posted Date: April 25th, 2022

DOI: https://doi.org/10.21203/rs.3.rs-1535339/v1

Abstract

Background

Metastasis is a major obstacle in treatment of cervical cancer (CC), and gene SPOP mediated regulatory effect is found to be involved in metastasis. However, its mechanisms have not been fully elucidated.

Methods

We performed proteomic sequencing, immunohistochemical staining (IHC) and scoring of SPOP in cancer tissues of 180 patients with 2009 FIGO stage IB1-IIA2 CC, and compared the expression of SPOP between pelvic lymph node (pLN) metastasis group and non-pLN metastasis group. We divided the data into two groups by SPOP expression, compared overall survival (OS) and relapse- free survival (RFS) of patients. In vitro, cells were carried out to determine whether SPOP overexpression or knockdown could affect the proliferation, cloning, wounding and Tanswell assays. Finally, the possible mechanism of pLN metastasis of CC was explored by analyzing the differences in the number and distance of various immune targets.

Results

SPOP is upregulated in CC with pLN metastasis and negatively associated with patient outcome. In vitro, SPOP promotes CC cell proliferation, invasion. Through further analysis, we found that there was no significant difference in the number of PD-1 and PD-L1 between the two groups, but the number of PD-1 in the range of PD-L1 100um was significantly increased.

Conclusion

This study presents that SPOP can inhibit the immune microenvironment by promoting PD-1 to move away from PD-L1, thereby promoting pLN metastasis of CC, resulting in worse OS and RFS in patients.

Background

Cervical cancer (CC) is the fourth most common cancer and the third leading cause of cancer-related deaths in women globally [1]. Metastasis, especially pelvic lymph node (pLN) metastasis, is a major challenge for CC treatment, as most CC-related mortality is caused by metastasis [2–5]. With the progress of diagnostic technology and therapeutic method, the clinical outcomes of CC have significantly improved [5–8]; however, there are currently no effective treatment options for preventing or inhibiting CC metastasis, in part because the molecular mechanisms that underlie CC invasion and pLN metastasis are not fully elucidated [9].

The nuclear speckle-type pox virus and zinc finger protein (SPOP), a representative substrate-recognition subunit (SRS) of cullin-RING E3 ligase 3 (CRL3, a member of CRL complex family) has been recognized as a dual role in the development and progression of human cancer, including lung, colon, gastric, prostate and liver cancers [10–16]. However, studies focusing on the role of SPOP in the development of CC are still lacking. In 2007, Byun et al. demonstrated that SPOP confers proapoptotic function in HeLa cells [17]. Until recently, Pang et al. demonstrated that CUL3/SPOP E3 ubiquitin ligase degraded DRAK1, thus promoting paclitaxel-resistant CC cells growth [18].

Traditional procedures have been used to elucidate the mechanism by regularly exploring molecular pathways [19–21]. However, due to the tissue-destructive nature of most of these methods, the spatial distribution and temporal distribution of immune milieu in situ will not be preserved [22]. Multiplex immunohistochemistry/immunofluorescence (m-IHC/IF) has emerged and provides high-throughput multiplex staining and further standardized quantitative analysis for highly efficient, reproducible and cost-effective tissue studies [22–26]. It can show up to seven targets simultaneously on a single slide. Afterwards, HALO (Indica Labs, Albuquerque, USA), an image analysis system not only can be used for quantitative tissue analysis, but also can reveal the spatial location of each target [27–31]. This will enable us to study the mechanism of tumor genesis and development from the perspective of spatial location, and expand the depth of our research.

In this study, we show that overexpression of SPOP is associated with pLN metastasis and clinical outcomes by inhibiting the immune microenvironment through promoting PD-1 to move away from PD-L1. This is the first time for us to explore the potential mechanism of CC pLN metastasis from the spatial relationship between molecules. It will provide a new direction for the future treatment of CC by exploring the mechanism of pLN metastasis of CC.

Methods

Patient Cohort

All procedures were ethically approved by the institutional Ethics Review Committee of Fudan University Shanghai Cancer center (FUSCC). Appropriate written informed consent was obtained from all patients prior to sample collection.

A retrospective cohort study was conducted in the Department of Gynecology Oncology, FUSCC, which included 180 patients with the 2009 FIGO stage IB1-IIA2 who underwent radical abdominal hysterectomy with or without bilateral salpingooophorectomy and pelvic ± para-aortic lymphadenectomy from 2009 to 2012. All the enrolled patients had undergone standard pelvic lymphadenectomy by experienced gynecological oncologist. All the microscopic slides including gene SPOP staining were reviewed and graded by the same professional gynecologic pathologist and were reconfirmed by another experienced gynecologic pathologist. All clinical records were retrospectively studied.

Proteomic Sequencing and Data Process

Proteomic sequencing was performed in 5 lymph node positive cervical cancer tissues and 5 lymph node negative cervical cancer tissues, and subsequent analysis was performed.

Immunohistochemical Staining (IHC)

IHC of SPOP was performed on the paraffin-embedded sections of 180 CC tissues. Slice thickness was set at 5 mm and 3 sections were selected from each specimen. Slides were rinsed and incubated with primary antibodies SPOP (1:100; Cell Signaling Technology). Subsequent antibody detection was carried out with a secondary antibody: Cy3-conjugated goat anti-rabbit (1:300; Wuhan Goodbio Technology CO., LTD.). The expression level of SPOP was determined by immunoreactive score (IRS) [32–34].

Cell Culture and Reagents

The human cervical cancer cell lines HeLa, SiHa, ME-180, MS751 were acquired from the American Type Culture Collection (ATCC), which were authenticated by short tandem repeat profiling. These cell lines were cultured at 5% CO2 and 37°C in high-glucose Dulbecco's modified Eagle's medium (DMEM; Gibco, USA), containing 10% fetal bovine serum (FBS; Gibco, USA) and 1% penicillin-streptomycin (Gibco, USA).

Plasmids

The SPOP overexpression plasmid was constructed by cloning the cDNA into the PGMLV-CMV-EF1-ZsGreen1-T2A-Puro vector (System Biosciences, CA, USA). Plasmids carrying shRNAs targeting SPOP were generated using the U6-MCS-CMV-ZsGreen1-PGK-Puro vector (System Biosciences, CA, USA). The siRNAs and matched empty vector controls were obtained from Lncbio (Shanghai, China). The SPOP shRNAs target sequence is as follows: shRNA1: GTAGCACCAACTCTCAGCTA, shRNA2: CCTCCGGCAGAAATGTCGAG, shRNA3: TGACTTCACCCATTTCCTCC.

RNA extraction and qRT-PCR

Total RNA was extracted from samples and cells using TRIzol reagent (Life Technologies, CA, USA), according to the manufacturer's protocol. qRT-PCR was conducted using TB Green PCR Master Mix (TaKaRa, Dalian, China) inanABI7900HT Real-Time PCR system (Applied Biosystems, USA). The relative quantification was normalized to b-actin with the 2CT formula. The primers used for qRT-PCR are listed as follows: β-actin-F: AATGGACTATCATATGCTTACCGTAACTTGAAAGTATTTCG; β-actin-F: CTTTAGTTTGTATGTCTGTTGCTATTATGTCTACTATTCTTTCC; SPOP-F: GCCCCGTAGCTGAGAGTTG; SPOP-R: ACTCGCAAACACCATTTCAGT.

Western Blot Analysis

Western blotting was performed as our previously described [35].

CCK-8 Assay

Cells were seeded and cultured into 96-well plates overnight. At 1, 2, 3, 4, 5 day, 10ul cell counting kit-8 solution (MedChem Express, Monmouth Junction, NJ, USA) was added into each well, followed by further

incubation at 37°C. After 1 h, the absorbance was measured at 450 nm wavelength to assess cell proliferation ability [36].

Colony Formation Assay

Cells were seeded and cultured in 6-well plates at a density of $1*10^3$ cells/well. During this period, the medium should be changed as needs. After two weeks, cells were fixed with 4% paraformaldehyde (PFA, Sangon Biotech) and stained with 0.1% crystal violet (Beyotime) for 15 minutes [37].

Cell Cycle Assay

Cells were seeded and cultured into 6-cell plates at a density of $3*10^5$ cells/well. After 2 days, cells for cell cycle analysis were digested with trypsin (Hyclone), washed with phosphate-buffered saline (PBS) for three times, and fixed into 70% ethanol overnight at -20 ℃. Then cells were centrifuged at 500g for 20 minutes, washed three times with cold PBS. After treated with RNase A (0.1mg/ml) and propidium iodide (PI, 0.05mg/ml) for 15min in the dark. Flow cytometry were applied in the tested [38].

Cell Migration and Invasion Assays

For wound healing assays, cells were cultured in 6-well plates and scratched with 1ml pipette tip and the wounds were photographed at 0 h and 36 h. The relative migration ratio was calculated [39, 40].

For migration assays, a 24-well plate with Transwell chambers (8um pore size, Coring) was applied. A serum concentration difference is formed between the upper and lower chambers (upper: 10%FBS; lower: FBS-free). $4*10^4$ cells were cultured into the upper chamber containing solubilized extracellular matrix (ECM) -coated members, as previously described manufacturer's instructions (Coring Matrigel invasion assay; USA) for 24h. The cells on the lower surface of the chambers were fixed with 4% PFA for 15 minutes and stained with 0.1% crystal violet for 15 minutes [41, 42].

Making Tissue Microarray (TMA)

The 180 CC patients' tissues (in situ) were prepared into TMA as previously described [43].

M-IF Staining Protocol

Opal 7-colour kit (NEL811001KT, PerkinElmer) was used for mIF. TMAs were dewaxed and rehydrated. In the first step, antigen was retrieved at 125 ℃ for 3 min and then cooled to room temperature (RT). Washed with TBST three times for 5min, incubated in H_2O_2 for 10 min. Repeated washed and blocked with blocking buffer. Primary antibody, PDL-1 (ab237726, abcam, 1:500, dye 480) was incubated at RT for 30min. Slides were washed and an HRP-conjugated secondary antibody was incubated at RT for 10min. TSA dye (1:100) was applied for 10min after washes. The procedures were repeated six times using the following antibodies, CD3 (ab16669, abcam, 1:200, dye 690; used as T lymphocyte cell marker), CD8 (ab93278, abcam, 1:100, dye 570; used as cytotoxic T cell marker), CD56 (ab75813, abcam, 1:500, dye 620; used as NK cell marker), CD68 (ab213363, 1:1000, abcam, dye 780; used as pan-macrophage marker), programmed death-1 (PD-1) (ab237728, abcam, 1:300, dye 520), programmed death ligand-1

(PD-L1) (ab237726, 1:500, dye 480). Secondary antibodies anti-mouse (NEF822001EA, PerkinElmer) or anti-rabbit (NEF812001EA, PekinElmer) were used at a 1:1000 dilution [22, 44, 45].

Further analysis by HALO system, we can quantify the number of six immune targets and the spatial position relationship between them [45].

Half Maximal Inhibitory Concentration (IC50)

Cells ($4*10^3$ cells/well) were seeded and cultured into 96-well plates overnight. At 1 day, PD-1 was treated with different concentrations (0, 0.0625mg/ml, 0.125mg/ml, 0.25mg/ml, 0.5mg/ml, 1mg/ml, 2mg/ml, 4mg/ml, 8mg/ml). At 2 day, 10ul cell counting kit-8 solution (MedChem Express, Monmouth Junction, NJ, USA) was added into each well, followed by further incubation at 37°C. After 1 h, the absorbance was measured at 450 nm wavelength to assess cell proliferation ability [36].

Statistical Analysis

Statistical analysis was performed with IBM SPSS 23.0, Graphpad Prism 8 and R language. Comparisons between two conditions were based on two-sided Student's test. The results of all statistical analyses were reported as p values from two-tailed tests, and $P \leq 0.05$ was judged to be statistically significant (*****$P \leq 0.05$, ****** $P \leq 0.01$, and ******* $P \leq 0.001$).

Results

Patient Characteristics

The study cohort contained 180 cases of CC with high quality TMA. The median age of the patients was 46 years (95% Confidence Interval (CI): 23–71 years). The histological diagnosis was all squamous cell carcinoma and based on the FIGO 2009 guidelines, thirty-nine (43.3%) subjects were stage IB, fifty-one (56.7%) subjects were stage IIA. The median follow-up time was 123 months (95% CI: 107.28-138.72 months) while seven (7.8%) subjects died and thirteen (14.4%) subjects relapsed.

SPOP is frequently upregulated in CC with pLN metastasis and negatively associated with patient outcome

We analyzed the expression of SPOP in CC with pLN metastasis or without pLN metastasis in our center. Through proteome sequencing of two groups, we found that SPOP protein was significantly increased in the positive-group ($|FC| \geq 2.5$) (Fig. 1A). Additionally, the SPOP IHC scores (IHC score 1: Low group; IHC score 2 and 3: High group) can reach 1.52 ± 0.091 in the pLN-negative group, 2.04 ± 0.12 in the pLN-positive group (pLN-negative versus pLN-positive, $P < 0.01$) ($P = 0.0005$) (Fig. 1B). The above data suggest that SPOP may promote pLN metastasis in CC.

Furthermore, we applied the information of our center to group the patients by SPOP expression level. High SPOP levels (score 3) were markedly associated with an improved overall survival (OS; HR = 0.019 (0.015–0.029), P = 0.042) and relapse-free survival (RFS; HR = 0.093 (0.012–0.715), P = 0.022) (Fig. 1CD).

These data suggest that a higher-scoring SPOP expression will have considerably worse OS and RFS in CC.

SPOP promotes CC cell proliferation in vitro

Firstly, we established stable cell lines by knocking out SPOP or overexpressing SPOP. Verification is then performed at the protein and RNA levels (Fig. 2AB).

To further determined the tumor-promoting effect of SPOP on cell proliferation, we measured the expression levels of SPOP in various CC cell lines. Based on high endogenous expression of SPOP in HeLa and SiHa cells, we designed and synthesized two independent small hairpin RNAs (shRNAs) to effectively reduce SPOP RNA level, whereas ME-180 and MS751, with low endogenous SPOP expression levels, were transfected with lentivirus, containing SPOP sequence within the PGMLV vector to generate stable overexpressed cell lines. As showed in the results, SPOP knockdown significantly suppressed HeLa and SiHa cell proliferation ability, whereas SPOP overexpression significantly promoted ME-180 and MS751 cell proliferation ability (Fig. 2C). In addition, knockdown or overexpression of SPOP significantly decreased or increased, respectively, the colony-forming of CC cells (Fig. 2D).

To further evaluated whether SPOP has an effect on cell proliferation, we performed a cell cycle assay. The knockdown of SPOP significantly increased the percentage of cells in the G1 phase and decrease the percentage of cells in the S phase and G2 phase in HeLa cells (Fig. 3A). In SiHa cells, the same effect was achieved for SPOP knockdown in G1 and S phase cells, except that there was no statistical significance in G2 phase cells (Fig. 3B). In overexpression cells, upregulated SPOP can significantly decreased the cells percentage of G1 phase in ME-180 and MS751 cells, increased the cells percentage of G2 phase in ME180 cells and increased the cells percentage of S phase in MS751 cells (Fig. 3CD). The above data suggest that SPOP can promote the proportion of S phase and G2 phase cells, and reduce the proportion of G1 phase cells, thus promoting cell proliferation.

These above data have demonstrated that SPOP can promote the proliferation of CC cells.

SPOP promotes CC cell migration and invasion in vitro

The relationship between SPOP expression and distant metastasis encouraged us to further study whether SPOP can affect cell migration. Our results of wound-healing assays showed that shRNA-mediated SPOP knockdown suppressed the migration of HeLa and SiHa cells (Fig. 4A) but that SPOP overexpression significantly promoted ME-180 and MS751 cells migration (Fig. 4B).

Moreover, the Transwell assay showed that the invasion was suppressed when SPOP was silenced (Fig. 4C). Conversely, the promoting effect of SPOP on the invasion ability of ME-180 and MS751 cells was confirmed by SPOP overexpression (Fig. 4D). Overall, these data have demonstrated that SPOP can promote CC cells migration and invasion.

SPOP may promote migration by suppressing the spatial proximity between PD-1 and PDL-1

By HALO system, we analyzed the number and spatial location of six immune targets on TMA. We further divided the above data into two groups by the expression of SPOP (IHC score 1: Low group; IHC score 2 and 3: High group), compared the differences of various immune infiltrations and explored the potential mechanism of CC metastasis.

The number of PD-L1 expression was 6325 ± 1023 in the Low group, 6739 ± 808.3 in the High group (Low group versus High group, $P = 0.75$) (Fig. 5AB). The number of PD-1 expression was 6418 ± 822 in the Low group, 5009 ± 533.8 in the High group (Low group versus High group, $P = 0.13$) (Fig. 5CD). The difference between the two groups was not statistically significant, suggesting that SPOP did not affect PD-L1 and PD-1 expression. However, the average number of PD-1 within 100μm of PDL-1 was 2.56 ± 0.14 in the Low group, 1.75 ± 0.063 in the High group (Low group versus High group, $P < 0.01$) (Fig. 5EF).

Summary of the above data, PD-1 was significantly farther from PD-L1 in spatial distance with the increase of SPOP expression. This may be the potential mechanism of SPOP promoting CC metastasis.

SPOP can promote the immune tolerance of PD1 in vitro

The cells in the Control group and SPOP knockdown group were treated with different concentrations of PD-1, respectively, and the change of IC50 reflected that SPOP can promote PD-1 to be away from PD-L1, so as to achieve immune tolerance.

In HeLa cells, the IC50 can reach 3.63 ± 0.22 in the NC group, 2.26 ± 0.08 in the shRNA1 group, 2.18 ± 0.07 in the shRNA2 group (NC versus shRNA1, $P < 0.05$; NC versus shRNA2, $P < 0.05$) (Fig. 6A). The above data suggest that SPOP can promote PD-1 resistance in HeLa cells.

In SiHa cells, the IC50 can reach 3.217 ± 0.17 in the NC group, 1.901 ± 0.07 in the shRNA1 group, 1.869 ± 0.06 in the shRNA2 group (NC versus shRNA1, $P < 0.05$; NC versus shRNA2, $P < 0.05$) (Fig. 6B). The above data suggest that SPOP can promote PD-1 resistance in SiHa cells.

The above in vitro experiments further prove that SPOP can promote PD-1 drug resistance and achieve immune tolerance.

Relationship between SPOP and other immune targets

We further compared the differences in other immune indicators between the two groups, including CD3, CD8, CD56, and CD68, as well as the relationship between them and found that the differences were not statistically significant.

Discussion

Main findings and Interpretation

Previous studies have demonstrated that SPOP can suppress or promote tumorigenesis in a variety of malignancies, including lung, colon, gastric, prostate and liver cancers [10]. However, few studies

focusing on SPOP in the development of CC and only two reports also show dual effects [17, 18]. Traditional procedures have been used to elucidate the mechanism by regularly exploring such molecular pathways which would destroy the spatial structure[46, 47]. By mIF and HALO system, their spatial orientation interrelation of immune cells and immune markers would be preserved [22, 48]. Through a series of experiments, we demonstrated for the first time that SPOP promotes CC pLN metastasis by promoting PD-1 away from PD-L1.

Begin with this study, we found that the expression of SPOP is increased in CC with pLN-positive group compared with pLN-negative group. This suggests that SPOP may be associated with pLN metastasis in CC. Secondly, further analysis found that the High-SPOP group had relatively poor OS and RFS. In conclusion, these results have demonstrated that SPOP is upregulated in CC with pLN metastasis and negatively associated with patient outcomes.

Next and most importantly, we need to conduct in vitro experiments to prove a causal relationship between SPOP and CC cells migration and invasion. We showed in vitro that knockdown or overexpression of SPOP can significantly inhibit or promote, respectively, CC cell proliferation, cloning, cell cycle, wound healing and Transwell assays. These data suggest that SPOP can promote the migration and invasion of CC cells.

Finally, we analyzed the immune network environment of CC TMA again to find the potential mechanism of pLN metastasis. Through in-depth analysis, it was found that there was no significant difference in the number of PD-1 and PD-L1 between the two groups, but the number of PD-1 in the range of PD-L1 100um was significantly increased, indicating that the spatial distance between PD-1 and PD-L1 was further apart with the increase of SPOP.

To further prove this theory, we compared the Control group and SPOP knockdown group with different concentrations of PD-1 in HeLa and SiHa cell lines in vitro, and found that knocking down SPOP could significantly reduce the IC50 value of PD-1. This suggests that SPOP can promote PD-1 resistance in CC cells. It is proved that SPOP can achieve immune tolerance by promoting PD-1 to keep away from PD-L1.

These data suggest that SPOP may promote pLN metastasis by promoting PD-1 away from PD-L1 to inhibit immune microenvironment.

Limitations

We should further prove the causal relationship between SPOP and CC pLN metastasis in animals and verify the transfer mechanism in vivo.

Conclusion

In conclusion, SPOP can inhibit the immune microenvironment by promoting PD-1 to move away from PD-L1, thereby promoting pLN metastasis of CC, resulting in worse OS and RFS in patients. This is a typical process of deep clinical and basic cross-fusion validation exploration. Our study started from

clinical tissue data, proved causality on cells in vitro, and then returned to clinical samples to explore the potential causes of pLN metastasis through spatial location relationship from mIF, finally performing validation in vitro (Fig. 7). This will expand our understanding of CC progress and shed light on therapeutic targets for CC.

Declarations

Funding

This work was supported, in part, by grants from the Beijing Kanghua Foundation for the Development of Traditional Chinese and Western Medicine (KH-2021-LLZX-037).

Author Contributions

JC W, QH G, and J Z: Conceptualization, Data curation, Investigation, Writing - original draft. Y W: Conceptualization, Data curation, Investigation, Writing - original draft, Formal analysis, Methodology, Resources, Software, Validation, Visualization. SY C, SM W: Conceptualization, Funding acquisition, Project administration, Supervision, Writing - original draft, Writing - review & editing. XZ J, J Z, XH W: Conceptualization, Funding acquisition, Project administration, Supervision, Writing - original draft, Writing - review & editing.

Conflict of Interest

The authors declare no conflict of interest.

Ethics Approval and Consent to Participate

All study surgical procedures and experiment protocols have been approved by the Ethics Committee of Experimental Research, Shanghai Medical College, Fudan University. All participants have been informed the potential risks and benefits and each patient has signed the informed consent form.

Data Availability Statement

The data that support the results of this study are available from the corresponding author upon reasonable request.

References

1. Sung H, et al. Global Cancer Statistics 2020: GLOBOCAN Estimates of Incidence and Mortality Worldwide for 36 Cancers in 185 Countries. CA Cancer J Clin. 2021;71(3):209–49.
2. Gong Y, et al. MiR-29a inhibits invasion and metastasis of cervical cancer via modulating methylation of tumor suppressor SOCS1. Future Oncol. 2019;15(15):1729–44.

3. Diaz JP, et al. Sentinel lymph node biopsy in the management of early-stage cervical carcinoma. Gynecol Oncol. 2011;120(3):347–52.
4. Stevanovic S, et al. Complete regression of metastatic cervical cancer after treatment with human papillomavirus-targeted tumor-infiltrating T cells. J Clin Oncol. 2015;33(14):1543–50.
5. Kidd EA, et al. Lymph node staging by positron emission tomography in cervical cancer: relationship to prognosis. J Clin Oncol. 2010;28(12):2108–13.
6. Cheng X, et al. The prognosis of women with stage IB1-IIB node-positive cervical carcinoma after radical surgery. World J Surg Oncol. 2004;2:47.
7. Tsai CS, et al. The prognostic factors for patients with early cervical cancer treated by radical hysterectomy and postoperative radiotherapy. Gynecol Oncol. 1999;75(3):328–33.
8. Cho Y, et al. Tumor-related leukocytosis is associated with poor radiation response and clinical outcome in uterine cervical cancer patients. Ann Oncol. 2016;27(11):2067–74.
9. Hata M, et al. Radiation therapy for pelvic lymph node metastasis from uterine cervical cancer. Gynecol Oncol. 2013;131(1):99–102.
10. Song Y, et al. The emerging role of SPOP protein in tumorigenesis and cancer therapy. Mol Cancer. 2020;19(1):2.
11. Clark A, Burleson M. SPOP and cancer: a systematic review. Am J Cancer Res. 2020;10(3):704–26.
12. Shi Q, et al. Prostate Cancer-associated SPOP mutations enhance cancer cell survival and docetaxel resistance by upregulating Caprin1-dependent stress granule assembly. Mol Cancer. 2019;18(1):170.
13. Dai X, et al. Prostate cancer-associated SPOP mutations confer resistance to BET inhibitors through stabilization of BRD4. Nat Med. 2017;23(9):1063–71.
14. Cuneo MJ, Mittag T. The ubiquitin ligase adaptor SPOP in cancer. FEBS J. 2019;286(20):3946–58.
15. Zhang P, et al. Intrinsic BET inhibitor resistance in SPOP-mutated prostate cancer is mediated by BET protein stabilization and AKT-mTORC1 activation. Nat Med. 2017;23(9):1055–62.
16. Tang Z, et al. ATR Inhibition Induces CDK1-SPOP Signaling and Enhances Anti-PD-L1 Cytotoxicity in Prostate Cancer. Clin Cancer Res. 2021;27(17):4898–909.
17. Byun B, Tak H, Joe CO. BTB/POZ domain of speckle-type POZ protein (SPOP) confers proapoptotic function in HeLa cells. BioFactors. 2007;31(3–4):165–9.
18. Pang K, et al. Degradation of DRAK1 by CUL3/SPOP E3 Ubiquitin ligase promotes tumor growth of paclitaxel-resistant cervical cancer cells. Cell Death Dis. 2022;13(2):169.
19. Pouliot F, Johnson M, Wu L. Non-invasive molecular imaging of prostate cancer lymph node metastasis. Trends Mol Med. 2009;15(6):254–62.
20. Kawada K, Taketo MM. Significance and mechanism of lymph node metastasis in cancer progression. Cancer Res. 2011;71(4):1214–8.
21. Karaman S, Detmar M. Mechanisms of lymphatic metastasis. J Clin Invest. 2014;124(3):922–8.
22. Tan WCC, et al. Overview of multiplex immunohistochemistry/immunofluorescence techniques in the era of cancer immunotherapy. Cancer Commun (Lond). 2020;40(4):135–53.

23. Zou J, et al. Genetic alterations and expression characteristics of ARID1A impact tumor immune contexture and survival in early-onset gastric cancer. Am J Cancer Res. 2020;10(11):3947–72.
24. Nearchou IP, et al. Spatial immune profiling of the colorectal tumor microenvironment predicts good outcome in stage II patients. NPJ Digit Med. 2020;3:71.
25. Jaffar J, et al. CXCR4(+) cells are increased in lung tissue of patients with idiopathic pulmonary fibrosis. Respir Res. 2020;21(1):221.
26. Ozbek B, et al. Multiplex immunohistochemical phenotyping of T cells in primary prostate cancer. Prostate. 2022;82(6):706–22.
27. Hainaut P, Plymoth A. Targeting the hallmarks of cancer: towards a rational approach to next-generation cancer therapy. Curr Opin Oncol. 2013;25(1):50–1.
28. Toki MI, et al. High-Plex Predictive Marker Discovery for Melanoma Immunotherapy-Treated Patients Using Digital Spatial Profiling. Clin Cancer Res. 2019;25(18):5503–12.
29. Morrison LE, et al. Brightfield multiplex immunohistochemistry with multispectral imaging. Lab Invest. 2020;100(8):1124–36.
30. Widodo SS, et al. Toward precision immunotherapy using multiplex immunohistochemistry and in silico methods to define the tumor immune microenvironment. Cancer Immunol Immunother. 2021;70(7):1811–20.
31. Viratham Pulsawatdi A, et al. A robust multiplex immunofluorescence and digital pathology workflow for the characterisation of the tumour immune microenvironment. Mol Oncol. 2020;14(10):2384–402.
32. Specht E, et al. Comparison of immunoreactive score, HER2/neu score and H score for the immunohistochemical evaluation of somatostatin receptors in bronchopulmonary neuroendocrine neoplasms. Histopathology. 2015;67(3):368–77.
33. Hofmann M, et al. Assessment of a HER2 scoring system for gastric cancer: results from a validation study. Histopathology. 2008;52(7):797–805.
34. Beilner D, et al. Nuclear receptor corepressor (NCoR) is a positive prognosticator for cervical cancer. Arch Gynecol Obstet. 2021;304(5):1307–14.
35. Wang S, et al. Programmed death ligand 1 promotes lymph node metastasis and glucose metabolism in cervical cancer by activating integrin beta4/SNAI1/SIRT3 signaling pathway. Oncogene. 2018;37(30):4164–80.
36. Zhang L, et al. H19 knockdown suppresses proliferation and induces apoptosis by regulating miR-148b/WNT/beta-catenin in ox-LDL -stimulated vascular smooth muscle cells. J Biomed Sci. 2018;25(1):11.
37. Liu F, et al. Sonic Hedgehog Signaling Pathway Mediates Proliferation and Migration of Fibroblast-Like Synoviocytes in Rheumatoid Arthritis via MAPK/ERK Signaling Pathway. Front Immunol. 2018;9:2847.

38. Zhang S, et al. circCELSR1 (hsa_circ_0063809) Contributes to Paclitaxel Resistance of Ovarian Cancer Cells by Regulating FOXR2 Expression via miR-1252. Mol Ther Nucleic Acids. 2020;19:718–30.
39. Mascharak S, et al. Multi-omic analysis reveals divergent molecular events in scarring and regenerative wound healing. Cell Stem Cell. 2022;29(2):315–27 e6.
40. Monika P, et al. Challenges in Healing Wound: Role of Complementary and Alternative Medicine. Front Nutr. 2021;8:791899.
41. Liu Z, et al. Hypoxia-induced up-regulation of VASP promotes invasiveness and metastasis of hepatocellular carcinoma. Theranostics. 2018;8(17):4649–63.
42. Yang P, et al. TCONS_00012883 promotes proliferation and metastasis via DDX3/YY1/MMP1/PI3K-AKT axis in colorectal cancer. Clin Transl Med. 2020;10(6):e211.
43. Glinsmann-Gibson B, et al. Recommendations for Tissue Microarray Construction and Quality Assurance. Appl Immunohistochem Mol Morphol. 2020;28(4):325–30.
44. Sharpe AH, Pauken KE. The diverse functions of the PD1 inhibitory pathway. Nat Rev Immunol. 2018;18(3):153–67.
45. Taube JM, et al., *The Society for Immunotherapy of Cancer statement on best practices for multiplex immunohistochemistry (IHC) and immunofluorescence (IF) staining and validation*. J Immunother Cancer, 2020. 8(1).
46. Wu H, et al. RACK1 promotes the invasive activities and lymph node metastasis of cervical cancer via galectin-1. Cancer Lett. 2020;469:287–300.
47. Shang C, et al. LNMICC Promotes Nodal Metastasis of Cervical Cancer by Reprogramming Fatty Acid Metabolism. Cancer Res. 2018;78(4):877–90.
48. Carbone A, et al. Optimizing checkpoint inhibitors therapy for relapsed or progressive classic Hodgkin lymphoma by multiplex immunohistochemistry of the tumor microenvironment. Cancer Med. 2019;8(6):3012–6.

Figures

Figure 1

SPOP is upregulated in CC with pLN metastasis and negatively associated with patient outcome. A The expression of 33 key proteins in our proteomic sequencing data from 5 pLN- positive CC tissues and 5 pLN- negative CC tissues are presented in heatmap. **B** The IHC scores of SPOP in the group of pLN positive CC was significantly higher than that in the group of pLN negative CC ($P < 0.01$). **C** A Kaplan-Meier analysis was performed to assess the associations between SPOP expression and the OS (p=0.042) and RFS (p=0.022) of patients with CC. Data are presented as mean ± SEM.

Figure 2

Effects of SPOP on the proliferation of cervical cancer cells in vitro. A qRT-PCR and (**B**) Western blot analyses of SPOP levels following SPOP knockdown and overexpression. **C** CCK-8 and **(D)** colony-formation were performed to assess the changes in the proliferation.

Figure 3

In vitro cell cycle assay. A In HeLa cells, cell cycle experiments showed that SPOP knockdown could significantly promote the proportion of G1 phase cells and reduce the proportion of S and G2 phase cells. **B** In SiHa cells, cell cycle experiments showed that SPOP knockdown could significantly promote the percentage of G1 phase cells and reduce the percentage of S phase cells. **C** In ME-180 cells, cell cycle experiments showed that overexpression of SPOP could significantly reduce the proportion of G1 phase cells and increase the proportion of G2 phase cells. **D** In MS751 cells, cell cycle experiments showed that overexpression of SPOP could significantly reduce the proportion of G1 phase cells and increase the proportion of S phase cells.

Figure 4

SPOP promotes CC cell migration and invasion in vitro. A Wound-healing assays showed that shRNA-mediated SPOP knockdown suppressed the migration of HeLa and SiHa cells. **B** SPOP overexpression significantly promoted ME-180 and MS751 cells migration. **C** The Transwell assay showed that the invasion was suppressed when SPOP was silenced. **D** The promoting effect of SPOP on the invasion ability of ME-180 and MS751 cells was confirmed by SPOP overexpression.

Figure 5

SPOP may promote migration by suppressing the spatial proximity between PD-1 and PDL-1. AB SPOP did not affect PD-L1 expression. **CD** SPOP did not affect PD-1 expression. **EF** PD-1 was significantly farther from PD-L1 in spatial distance with the increase of SPOP expression.

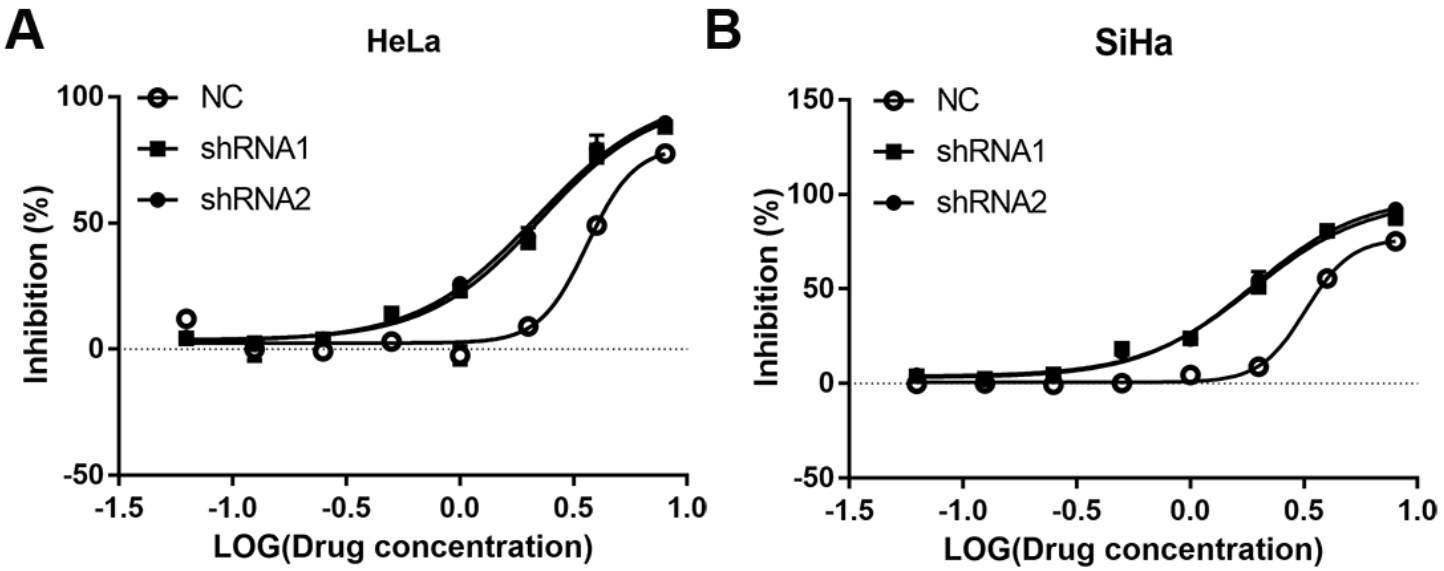

Figure 6

SPOP can promote the immune tolerance of PD1 in vitro. A The figure suggests that SPOP can promote PD-1 resistance in HeLa cells. **B** The figure suggests that SPOP can promote PD-1 resistance in SiHa cells.

Figure 7

Flow diagram (from 1 to 4). This flow chart shows the whole research idea. The first part introduces the source of SPOP and the meaning of studying SPOP. The second part verifies the causal relationship between SPOP and cervical cancer (CC) lymph node (pLN) metastasis from the cells level. Furthermore, according to the multiple immunofluorescence (mIF) and HALO analysis data of tissue microarray (TMA), SPOP can promote PD-1 to move away from PD-L1. Finally, IC50 was used to verify that SPOP knockdown could affect the immune tolerance of PD-1.

Supplementary Files

This is a list of supplementary files associated with this preprint. Click to download.

- Highlights.docx